How Individual Movement Response to Habitat Edges Affects Population Persistence and Spatial Spread

Gabriel Andreguetto Maciel[1] and Frithjof Lutscher[2,*]

1. Instituto de Física Teórica, Universidade Estadual Paulista, São Paulo, Brazil; 2. Department of Mathematics and Statistics, University of Ottawa, Ottawa, Canada

Submitted April 4, 2012; Accepted February 5, 2013; Electronically published May 15, 2013

Online enhancements: appendixes.

abstract: How individual-level movement decisions in response to habitat edges influence population-level patterns of persistence and spread of a species is a major challenge in spatial ecology and conservation biology. Here, we integrate novel insights into edge behavior, based on habitat preference and movement rates, into spatially explicit growth-dispersal models. We demonstrate how crucial ecological quantities (e.g., minimal patch size, spread rate) depend critically on these individual-level decisions. In particular, we find that including edge behavior properly in these models gives qualitatively different and intuitively more reasonable results than those of some previous studies that did not consider this level of detail. Our results highlight the importance of new empirical work on individual movement response to habitat edges.

Keywords: edge behavior, spatial heterogeneity, population dynamics, reaction-diffusion equations.

Introduction

Many empirical and theoretical studies have explored the effects of habitat fragmentation on various species, from plants and insects to birds and mammals (Shigesada et al. 1986; Debinski and Holt 2000; With 2002; Schtickzelle and Baguette 2003; Van Houtan et al. 2007; Dewhirst and Lutscher 2009). A salient feature of fragmented landscapes are edges, defined broadly as interfaces where landscape characteristics change abruptly (Lidicker 1999). Such edges can have several effects on population density and distribution (Ries et al. 2004), often related to individual movement behavior at these landscape features.

Novel experiments and technology provide insights and data on how individual movement characteristics change in response to edges. Schultz and Crone (2001) demonstrated such changes for a prairie butterfly (*Icaricia icarioides fenderi*) within a patch, outside of a patch, and near edges (see also Crone and Schultz 2008); edge behavior significantly increased residence time in a favorable patch. Ries and Debinski (2001) showed that a habitat specialist (*Speyeria idalia*) and generalist (*Danaus plexippus*) butterfly responded differently to different habitat edges and that the specialist returned more frequently to a favorable patch. Reeve et al. (2008) characterized movement rates of planthoppers (*Prokelisia crocea*) in three different habitat types and determined that individuals easily crossed edges between two types but not into unfavorable habitat. Such behavior is highly species specific; a parasitic wasp (*Anagrus columbi*) of these planthoppers shows behavior that is significantly different from that of its host at the same edges (Reeve and Cronin 2010). Movement of forest songbirds is impeded by gaps in the forest cover, and gap-crossing probability decreases with gap size (Creegan and Osborne 2005; Robertson and Radford 2009). Wolves and other large carnivores bias their movement toward forest edges and linear features, on which they travel farther and faster to increase their predation success (Whittington et al. 2005; McKenzie et al. 2012).

Connecting this wealth of information about individual movement to predictions about population-level outcomes such as extinction, persistence, and spread is a formidable task, and there is currently no coherent framework in place. Cellular automata have been used successfully to tackle some of these questions, most notably about dispersal distances, percolation thresholds, and spatial scales (With 2002). Such models can include detailed assumptions about species and landscapes, and they are easily accessible to direct numerical simulation and visualization. However, very few studies consider behavioral response to habitat edges (e.g., Chapman et al. 2007). Reaction-diffusion equations and their underlying random walk models have been applied successfully to spatial ecology (Cantrell and Cosner 2003), specifically for biological movement (Turchin 1998) and invasions (Andow et al. 1990). Shigesada et al. (1986) first studied persistence and

* Corresponding author; e-mail: flutsche@uottawa.ca.

Am. Nat. 2013. Vol. 182, pp. 42–52.
DOI: 10.1086/670661

invasions in patchy landscapes but did not consider individual behavioral response to habitat edges. Consequently, they arrived at the counterintuitive result that slow movement through unfavorable habitat patches could enhance population persistence, whereas fast movement there could decrease the rate of spread. Ludwig et al. (1979) considered the critical size of a single patch surrounded by less favorable matrix, also not incorporating behavior at habitat edges. Cantrell and Cosner (1999) modeled edge behavior and habitat preference using skew Brownian motion (Walsh 1978), which has the undesirable property that habitat edges can act as sources or sinks of individuals. More recently, Ovaskainen and Cornell (2003) modeled random walks across habitat edges, including habitat preference. Their framework was used to estimate movement parameters (Reeve et al. 2008; Reeve and Cronin 2010) and to determine occupancy times (Ovaskainen 2008).

Here, we jointly generalize the work of Ovaskainen and Cornell (2003)—and earlier Nagylaki (1976)—on edge behavior and integrate the results with classical reaction-diffusion models to assess the effects of edge behavior on population persistence and spread. We introduce our modeling framework in the next section, while giving detailed derivations in appendix A (app. A and B are available online). We reexamine the models by Shigesada et al. (1986) for periodically arranged patches and by Ludwig et al. (1979) for a single patch with behavioral response to edges included. We find that some predictions of both of these seminal models differ substantially when edge behavior is considered. Hence, including edge behavior proves essential to correctly understand population-level patterns. We proceed to address some questions on behavior and patch preference that could not be considered in the existing reaction-diffusion framework. In the discussion, we give biological interpretations and identify future challenges for empirical and theoretical work.

Models and Methods

Growth and Diffusion in Heterogeneous Landscapes

In reaction-diffusion models, individual movement is described by a random walk; reproduction occurs locally on the same timescale (Okubo and Levin 2001; Cantrell and Cosner 2003). The equation for the population density $u(t, x)$ at time t and location x in a homogeneous one-dimensional habitat is

$$\frac{\partial u}{\partial t} = D\frac{\partial^2 u}{\partial x^2} + f(u), \tag{1}$$

where D is the diffusion coefficient and f describes net growth. Fisher (1937) studied this equation in genetics; Skellam (1951) applied it to ecology. The population described by equation (1) persists in an infinite landscape if $f'(0) > 0$ and, with logistic growth $f(u) = ru(1 - u)$, spreads with speed $c^* = 2(Dr)^{1/2}$ when introduced locally (Weinberger 1982).

Skellam (1951) and Kierstead and Slobodkin (1953) considered a single "good" patch, $[-L/2, L/2]$, surrounded by an inhospitable environment and posed the "minimal patch size problem" of how large a good patch has to be to support a population. The answer depends on movement behavior at the boundary. The worst-case scenario that individuals leave the patch upon reaching the boundary and never return is modeled by "hostile" boundary conditions $u(\pm L/2, t) = 0$. Together with the logistic growth term, this yields the minimal size $L^* = \pi(D/r)^{1/2}$. Conversely, if individuals never cross the boundary the population can persist on a patch of any size; this scenario is modeled by "no-flux" conditions $\partial u/\partial x(\pm L/2, t) = 0$. More realistically, density and flux at the boundary are related by Robin's boundary conditions (Fagan et al. 1999)

$$\frac{\partial u}{\partial x} + \beta u = 0, \tag{2}$$

which reflect movement behavior at the boundary (Van Kirk and Lewis 1999; Lutscher et al. 2006). For $\beta = 0$ ($\beta \to \infty$), one retrieves no-flux (hostile) conditions, respectively.

Natural landscapes consist of patches of different quality. Growth conditions vary between patches, and movement behavior changes according to habitat features. Accordingly, in model (1) diffusivity D and parameters in function f are constant within a patch but differ between patches. Choosing logistic growth, the density u_i on patch type i satisfies

$$\frac{\partial u_i}{\partial t} = D_i\frac{\partial^2 u_i}{\partial x^2} + u_i(r_i - \mu_i u_i). \tag{3}$$

Mathematically, we require interface conditions that relate population density and flux between adjacent patches, similar to condition (2) at a boundary. Ecologically, these conditions should reflect movement behavior and patch preferences.

Behavior at Interfaces

Previous authors assumed that population density and flux are continuous across an interface (Ludwig et al. 1979; Shigesada et al. 1986; Cruywagen et al. 1996; Lutscher et al. 2006; Artiles et al. 2008; Vergni et al. 2012). Flux continuity is a natural condition that implies that all individuals who leave one patch enter the adjacent patch; none are introduced or lost at the interface. Continuity of den-

sity may be mathematically reasonable but may (Nagylaki 1976) or may not (Ovaskainen and Cornell 2003) be ecologically correct.

Jointly generalizing the work of these authors, we model individual movement within each patch as a random walk with a given time and space step. Upon reaching the interface between patch 1 and patch 2, say, individuals choose to move to patch i with probability α_i, where $\alpha_1 + \alpha_2 \leq 1$. We can interpret parameters α_j as a measure of habitat preference. After applying the usual parabolic scaling, we find that the flux is continuous at an interface but that the density may be discontinuous. More formally, if u_i and D_i denote the density and diffusion rate in patch i, then the interface conditions read (see app. A, sec. A1, for details)

$$u_1 = ku_2 \text{ and } D_1 \frac{\partial u_1}{\partial x} = D_2 \frac{\partial u_2}{\partial x}. \tag{4}$$

Parameter k measures the discontinuous "jump" in density at the interface. Its value depends on habitat preference and on the particular assumptions about individual movement in either patch. In this work, we shall consider the following three scenarios.

Scenario 1. If individuals move from the interface into patch i at the same rate as they move within patch i, we obtain (Nagylaki 1976)

$$k = 1 \text{ or } u_1 = u_2 \quad \text{(continuous density)}. \tag{5}$$

This scenario may correspond to an abrupt change in land cover (e.g., dense underbrush versus open grassland) and individuals whose movement rate is strongly affected by these physical differences. It implies that individuals enter patches at a low rate if they move slowly in these patches. Foraging theory, however, suggests that individuals should move slowly in favorable patches and should enter these patches with high probability. Scenario 1 cannot accommodate these characteristics.

Scenario 2. Suppose individuals move from the interface into patch 1 with probability $\alpha_1 = \alpha$ and into patch 2 with probability $\alpha_2 = 1 - \alpha$, independently of the movement probability inside patch i. If the step sizes in different patches may differ but the movement rates may not, then we obtain (Ovaskainen and Cornell 2003)

$$k = \frac{\alpha}{1 - \alpha} \sqrt{\frac{D_2}{D_1}} \quad \text{(discontinous density 1)}. \tag{6}$$

Here, an individual chooses a patch according to some features and inside a patch adjusts step sizes to, say, the distribution of host plants or other characteristics. In particular, the individual can choose to move into favorable habitat with high probability and then make small steps there to increase residence time.

Scenario 3. In the same setup as scenario 2, if an individual adjusts the probability of movement inside a patch but keeps the step size constant, then we arrive at

$$k = \frac{\alpha}{1 - \alpha} \frac{D_2}{D_1} \quad \text{(discontinous density 2)}, \tag{7}$$

as in Ovaskainen and Cornell (2003). Here, the individual waits longer between steps in good patches than in unfavorable ones but moves by the same distance if it moves at all.

In scenarios 2 and 3, we observe two mechanisms for a discontinuity in density: habitat preference ($\alpha \neq 0.5$) and unequal movement rates ($D_1 \neq D_2$). A preference for one of the two patches should lead to a significantly higher density of individuals in the preferred patch. In fact, $\alpha/(1 - \alpha)$ is an increasing function of α and equals unity when there is no habitat preference ($\alpha = 0.5$). But higher movement rate in one patch also leads to a lower population density near the interface in that patch. As individuals move at a high rate, they move away from the interface and spread out faster, so that the density near the interface declines. Previous authors, mentioned above, did not consider habitat preference but used continuous density conditions at the interface also for different diffusion rates in the two patches. As we explore population patterns resulting from these different interface conditions, the most striking differences between previous results and ours emerge in how the diffusion rates influence persistence and spread.

Results

Persistence Condition

We consider a periodically alternating landscape of favorable (type 1) and unfavorable (type 2) patches of length L_1 and L_2, respectively (Shigesada et al. 1986). Since persistence conditions emerge at low density, we study the linearized equations. We assume that the growth rate in favorable patches is positive ($r_1 > 0$) and larger than that in unfavorable patches ($r_1 > r_2$). When unfavorable patches are sinks ($r_2 < 0$), we ask for conditions under which the population can still persist at the landscape level, depending on interface behavior. In nondimensional quantities,

$$T = r_1 t, \quad X = \sqrt{\frac{r_1}{D_1}} x, \quad D = \frac{D_2}{D_1},$$

$$r = \frac{r_2}{r_1}, \quad S_i = L_i \sqrt{\frac{r_1}{D_1}},$$

the linear model reads (see app. A, sec. A2)

$$\frac{\partial U_1}{\partial T} = \frac{\partial^2 U_1}{\partial X^2} + U_1 \quad \text{(in favorable patches)}, \tag{8}$$

$$\frac{\partial U_2}{\partial T} = D\frac{\partial^2 U_2}{\partial X^2} + rU_2 \quad \text{(in unfavorable patches)}. \tag{9}$$

At the interfaces, we impose conditions (4).

Following the analysis in Shigesada et al. (1986), we study the stability of the zero solution and find the persistence boundary as the implicit relationship (note $r < 0$)

$$k\tan\left(\frac{S_1}{2}\right) = \sqrt{-rD}\tanh\left(\sqrt{\frac{-r}{D}}\frac{S_2}{2}\right). \tag{10}$$

We illustrate a few cases of how parameters and interface conditions affect population persistence. The maximum size of unfavorable patches that allows persistence is an increasing function of the growth rate in those patches, all other things being equal (fig. 1*A*, 1*B*). This increasing relationship holds for all three interface conditions. When $D > 1$, the maximal length of an unfavorable patch is smallest for $k = 1$ and largest for k as in condition (7) (fig. 1*A*). When individuals move more slowly in unfavorable habitat, the ordering is reversed (fig. 1*B*). The minimal size of favorable patches that enables persistence increases with the size of the unfavorable patches (fig. 1*C*). This relationship also holds for all three interface conditions. The minimum size of favorable patches is smallest for k as in condition (7) and largest for continuous density, provided $D > 1$. When $D < 1$, the situation is again reversed (app. A, sec. A2; fig. A1).

Persistence conditions as a function of diffusivity in unfavorable patches differ significantly among the three interface conditions. For continuous density, the maximum size of unfavorable patches decreases as diffusivity increases. In fact, there is a critical diffusivity below which the population persists for arbitrarily large unfavorable patches (Shigesada et al. 1986). The two other interface conditions predict that the maximum unfavorable patch size increases with diffusivity D, either in a decelerating fashion (interface condition [6]) or even in an accelerating fashion (interface condition [7]; see fig. 1*D*).

The amount of favorable habitat required for persistence is a decreasing function of preference for favorable patches, since individuals are less likely to leave a favorable patch.

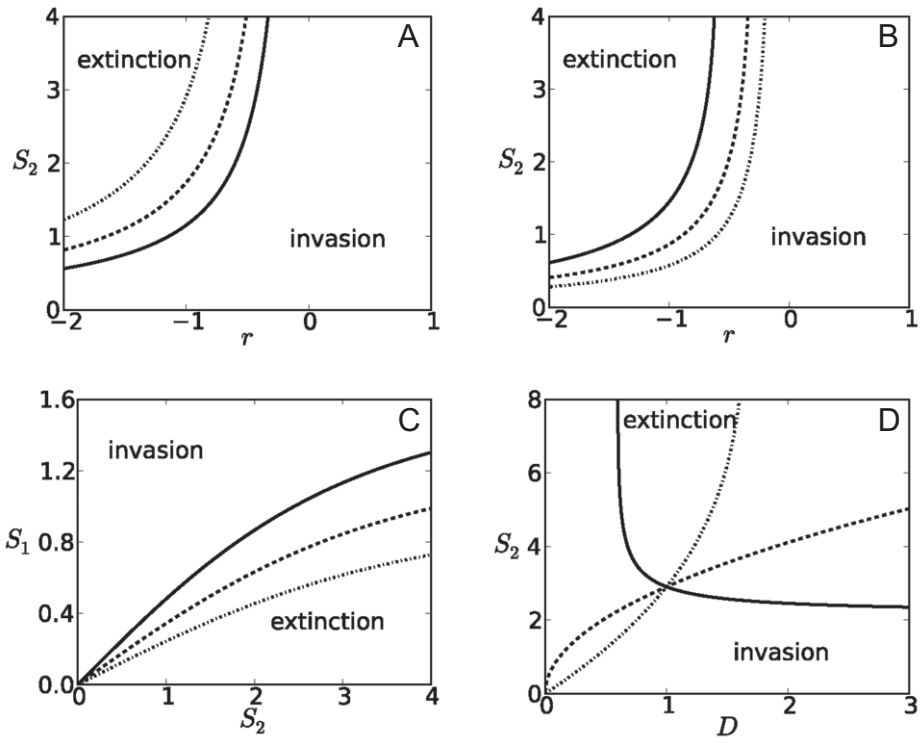

Figure 1: Persistence conditions (10) as a function of unfavorable patch size S_2 and growth rate in an unfavorable patch r (*A*, *B*), patch sizes S_1 and S_2 (*C*), and unfavorable patch size S_2 and diffusivity D (*D*). The three curves correspond to $k = 1$ (solid curve), k as in condition (6) (dashed curve), and k as in condition (7) (dash-dot curve). Parameters are as follows: *A*, $D = 2$ and $S_1 = 1$; *B*, $D = 0.5$ and $S_1 = 1$; *C*, $D = 2$ and $r = -0.5$; and *D*, $S_1 = 1$ and $r = -0.5$. We assume that individuals show no habitat preference, so that $\alpha = 0.5$.

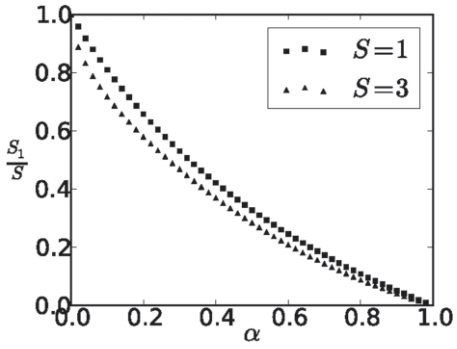

Figure 2: Persistence boundary as a function of habitat preference. The fraction of favorable habitat (S_1/S, where $S = S_1 + S_2$) required for persistence decreases with strength of preference (α). Fixed parameters are $D = 1$ (so that the discontinuous conditions are identical) and $r = -0.5$.

Conversely, the maximum length of unfavorable habitat that allows for persistence increases with preference for good habitat. If preference for favorable habitat is large enough, a population persists even for extremely long unfavorable patches (fig. 2).

Focal Patch Surrounded by Matrix Habitat

As a special case, we consider a single focal patch of good habitat surrounded by a nonlethal matrix habitat (Ludwig et al. 1979). We obtain the minimal size required for persistence on this focal patch by taking the limit $S_2 \to \infty$ in equation (10) and solving for S_1 as

$$S^* = 2 \arctan\left(\frac{\sqrt{-rD}}{k}\right). \tag{11}$$

For a hostile matrix (i.e., $r \to -\infty$) one obtains, independently of k, the critical value $S^* = \pi$, which is the threshold for hostile boundary conditions (Skellam 1951).

The qualitative behavior of S^* with respect to parameter r is independent of k; its dependence on the diffusion rate differs strikingly between the three cases for k. For continuous density, as considered by Ludwig et al. (1979), the critical length increases when diffusivity in the matrix increases; in the discontinuous 2 scenario the critical length decreases as diffusivity in the matrix increases, and in the discontinuous 1 scenario the result is independent of D (see fig. 3). The minimal patch size is a monotonically decreasing function of α, that is, higher preference for the focal patch implies a smaller critical patch size S^* (app. A, sec. A2; fig. A2).

Rate of Spatial Spread

When persistence is guaranteed, a locally introduced population will spread at an asymptotically constant speed, as was demonstrated numerically by Shigesada et al. (1986) and proved analytically by Weinberger (2002) for $k = 1$. The spread rate (c) and its dependence on parameters are arguably the most important quantities in the management of nonnative invasive species (Hastings et al. 2005). We illustrate how this speed depends on interface conditions and patch preference (for detailed calculations, see app. A, sec. A3).

Spread rate increases with growth rate in unfavorable patches (r; see fig. 4). If $D > 1$, the speed is slowest for continuous density and fastest for discontinuous condition (7); otherwise, the order is reversed (app. A, sec. A3; fig. A4). Points with $c = 0$ correspond to points on the persistence boundary in figure 1*A*. Curves for different S_2 intersect for some value $r < 1$. Hence, increasing the size of unfavorable patches can increase the spread rate if the movement rate is higher in these patches. Only if unfavorable patches have a sufficiently negative growth rate will increasing S_2 result in slower spread. The spread rate decreases with the size of unfavorable patches; the speed is highest for condition (7) and lowest for $k = 1$ if $D > 1$; the order is reversed if $D < 1$ (app. A, sec. A3; figs. A5, A6).

For both discontinuous interface conditions, spread rate increases with D. When diffusivity in unfavorable patches is small, the population does not spread. As the size of unfavorable patches increases, the threshold diffusivity for population spread also increases (figs. 5*B*, A3*B*). Again, zero spread rate corresponds to curves in the persistence plot (fig. 1*D*). For continuous interface conditions, how-

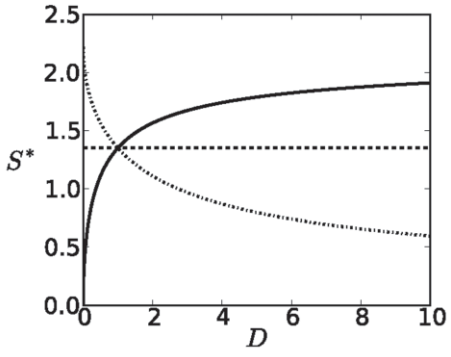

Figure 3: Minimal patch size S^* as a function of diffusivity in the matrix for the continuous density (solid curve), discontinuous 1 (dashed curve), and discontinuous 2 (dash-dot curve) interface conditions. We assume no habitat preference ($\alpha = 0.5$) and $r = -2$.

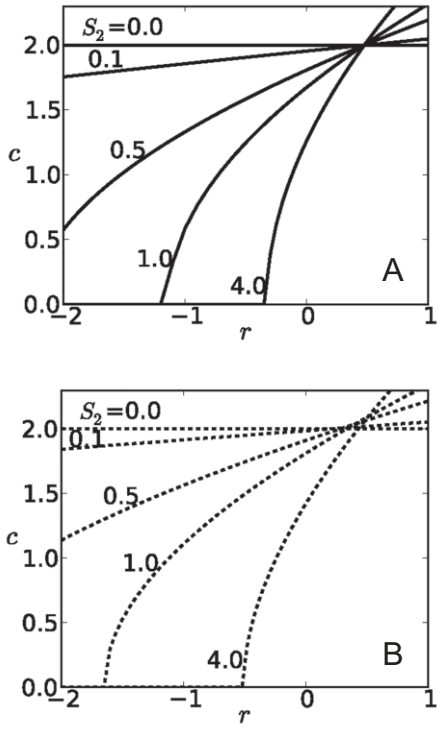

Figure 4: Spread rates as a function of intrinsic growth rate in the unfavorable patch. *A* corresponds to continuous density at interfaces ($k = 1$), and *B* corresponds to discontinuous density as in condition (6). Condition (7) is qualitatively similar to *B*, but speeds are higher (see app. A, sec. A3; fig. A3*A*). Parameters are $D = 2$ and $\alpha = 0.5$.

ever, the situation is strikingly different (fig. 5*A*). For any size of unfavorable patches, the spread rate is positive for small D. This finding reflects the result shown in figure 1*D*, that a population can persist in arbitrarily large unfavorable patches when D is small enough. When S_2 is large enough, the spread rate is a hump-shaped function of D (fig. 5*A*). Spatial spread halts for large enough D. For comparison, figures 5*A*, A4*A*, and A6*A* and are as in Shigesada et al. (1986).

Spread rate (c) depends on habitat preference (α) via two opposing mechanisms. Higher preference for favorable patches ($\alpha > 0.5$) increases the effective growth rate and thereby the spread rate. High preference for favorable patches also prevents individuals from leaving these patches and moving larger distances in space, which decreases the spread rate. If there is a strong preference for unfavorable patches (α near 0), the population cannot persist or spread, so that $c = 0$ (fig. 6). When the preference for favorable patches increases, the population becomes viable and spreads. The positive effect of α on the spread rate dominates for low to intermediate values of α; as preference for favorable patches becomes very strong ($\alpha \approx 1$), negative effects dominate, and c decreases to 0.

In the limit when the period of landscape heterogeneity (L) is small compared with the diffusion coefficients, we derive an explicit approximate expression for the spread rate. We expand the spread rate formula (eq. [A32]), sort by powers of L_1 and L_2, and obtain the approximation (in dimensional parameters) $c = 2(\langle D\rangle_H \langle r\rangle_A \hat{L}^2)^{1/2}$, where

$$\langle D\rangle_H = \frac{L_1 + L_2/k}{(L_1/D_1) + [(L_2/k)/(D_2/k^2)]},$$
$$\langle r\rangle_A = \frac{r_1 L_1 + r_2 L_2/k}{L_1 + L_2/k}, \tag{12}$$
$$\hat{L} = \frac{L_1 + L_2}{L_1 + L_2/k}$$

are the harmonic mean of the weighted diffusion constant and the arithmetic mean of the growth rate with weights L_1 and L_2/k, as well as the effective period.

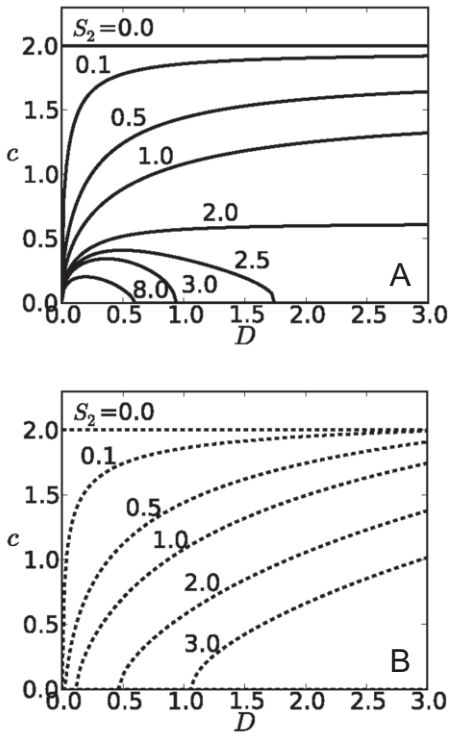

Figure 5: Spread rates as a function of diffusivity in unfavorable patches. *A* corresponds to continuous density at interfaces ($k = 1$), and *B* corresponds to discontinuous density as in condition (6). Condition (7) is qualitatively similar to *B* (see app. A, sec. A3; fig. A3*B*). Parameters are $r = -0.5$ and $\alpha = 0.5$.

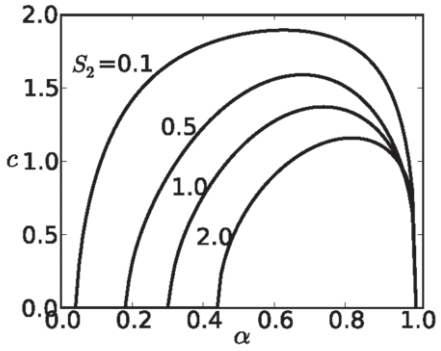

Figure 6: Spread rate as a function of preference for the favorable patches. The minimal value of α that allows spread increases as the size of the unfavorable patch size increases. Parameters are $D = 1$ (so that the two discontinuous conditions are the same) and $r = -0.5$.

Patch Preference Depends on Patch Attributes

We treated parameters as independent, but in reality dependencies and trade-offs exist. Entangling these effects and determining their net outcome provides important future applications of our model. We illustrate the power of our approach with a few examples.

Cantrell and Cosner (1999) considered a core habitat area surrounded by a buffer zone and allowed patch preference to depend on the difference in habitat quality (i.e., α was a function of $r_1 - r_2$; see app. B, sec. B1). This intuitively reasonable assumption leads to the surprising result that a larger core area is needed for persistence if the buffer is of high quality. This effect arises because a high-quality buffer attracts individuals who may subsequently leave the buffer and enter hostile surroundings; a poor-quality buffer, by contrast, creates an aversion to the unfavorable habitat, so that individuals remain in the good habitat and do not enter hostile surroundings. We reproduced these predictions in our model.

Alternatively, preference of a favorable patch may depend on the distance to the next favorable patch. For example, certain bird species that prefer wooded areas (e.g., for cover and protection) may cross open areas (and risk predation) if the nearest wooded area is within reasonable distance (in particular, if it is visible) but not when it is far away (Creegan and Osborne 2005; Robertson and Radford 2009). We explored this possibility by setting patch preference in the periodic environment to

$$\alpha(S_2) = \frac{\alpha_0(1 + \delta S_2)}{2\alpha_0 + \delta S_2} \tag{13}$$

with scaling parameter $\delta > 0$ (Cantrell and Cosner 1999). This function has the following desirable properties. Without bad patches, there is no preference ($\alpha(0) = 1/2$). Preference for favorable patches increases with the length of bad patches. For large unfavorable patches, preference is $\alpha_0 \in [1/2, 1]$, whereby 1 corresponds to no-flux conditions.

The critical length of favorable patches is a hump-shaped function of the size of bad patches (S_2). The two opposing mechanisms are as follows. An increase in S_2 leads to higher population loss in unfavorable patches and hence requires larger good patches for persistence. An increase in S_2 also decreases the probability of entering unfavorable patches and, hence, decreases mortality and allows for smaller S_1. At small S_2 the first effect dominates, whereas for larger S_2 the second effect is stronger (fig. 7). For the rate of spatial spread, increasing S_2 increases loss rates and thereby decreases speed. Increasing S_2 also increases α, which, as in figure 6, can increase or decrease speed when varied independently. The combined effect here acts to decrease the rate of spatial spread. However, higher retention in the favorable patches (i.e., larger α_0) gives higher spread rates, everything else begin equal (fig. 7).

Finally, we model a simple network of two favorable patches, each too small to sustain a population, joined by

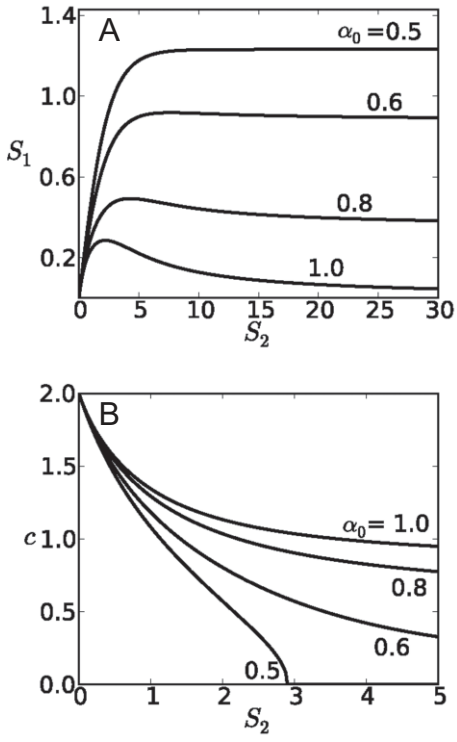

Figure 7: Persistence boundary (*A*) and invasion speed (*B*) when gap-crossing depends on gap size. Parameter values are $D = 1$ and $r = -0.5$.

a movement corridor, where net growth is negative (see app. B, sec. B2, for details and figures). All other things being equal, higher corridor mortality requires a shorter corridor for persistence (fig. B2). Individuals could offset high corridor mortality by faster movement. Choosing an appropriate increasing function (in dimensional terms, $D_2 = D_2(r_2)$, similar to eq. [13]) enhances persistence for discontinuous but not for continuous interface conditions. If instead patch preference increases with mortality (i.e., $\alpha = \alpha(r_2)$), two effects can occur. If maximal preference for favorable patches stays below a certain threshold, there is still a maximal distance between the two patches for persistence. If maximal preference is above the threshold, the population can persist even if the patches are very far apart (fig. B3). Preference for the good patch becomes so strong that few individuals leave. When individuals increase patch preference and movement rate in response to decreasing corridor quality, the combined effect increases population persistence even more (fig. B4).

Discussion

As a result of natural disturbances and human activities, landscapes increasingly consist of patches with different characteristics and suitability for different species. Whether a species persists or invades in such a landscape depends on how individuals move in these patches and how they respond to interfaces between different habitat types. A wealth of data is available on movement behavior in different habitat types (Ries and Debinski 2001; Schultz and Crone 2001; Whittington et al. 2005; Reeve et al. 2008), and there is a long history of studying habitat selection and patch preference of animals (Rosenzweig 1981; Brown 1988; Fryxell 2008; Beyer et al. 2010). Yet there was no modeling framework in place to combine this small-scale information and use it to predict population-scale patterns. Here, we extend the applicability of reaction-diffusion models to patchy landscapes by deriving appropriate interface conditions and thereby provide such a theoretical framework. We reanalyze several classical models in ecology and demonstrate how crucially important the correct implementation of interface behavior is to predicting population persistence and spread.

Our derivation of interface conditions generalizes the work by Ovaskainen and Cornell (2003), and it includes the conditions of Nagylaki (1976) as a special case. Hence, we can compare the resulting differences on a mechanistic basis. Specifically, in the absence of habitat preference, the rate of moving into a patch is 1/2 for the discontinuous conditions, whereas it equals the movement rate in that patch for continuous conditions. We first discuss the effect of differential movement rates, assuming no patch preference.

Effects of Movement Differentials

When individuals move faster in unfavorable habitat ($D > 1$), a population persists under considerably weaker conditions than those found by previous authors (figs. 1*A*, 1*D*, 3) and spreads faster through a heterogeneous landscape (figs. 4, A5), at least when unfavorable patches are sinks. When individuals move faster in favorable patches, these findings are reversed. The mechanism behind these results is that under continuous conditions individuals move into unfavorable habitat with a higher probability when $D > 1$ and with a lower probability when $D < 1$. This correlation between movement into and within a patch contradicts foraging theory, which suggests that individuals should move fast within but rarely into unfavorable patches. For example, if forest habitat is disrupted by highway, individuals should enter the highway at a low rate but once there move fairly quickly—a scenario that the continuous conditions cannot accommodate.

Empirically, individuals may move faster in unfavorable patches, trying to reach a favorable patch (Chapman et al. 2007; Reeve et al. 2008). Yet they may move more slowly because of physical obstructions or energy requirements. It is unclear which net effect would emerge (Hastings et al. 2005). We show that whether individuals move faster or slower in certain patches critically affects population patterns and needs to be considered carefully. This suggests that classifying patches by quality needs to include growth potential and individual movement ability (see also Fahrig 2007). For example, the growth potential of a species in agricultural and residential development could be similar, but agricultural land may present fewer obstacles to movement.

Two previous counterintuitive results do not appear here. A population cannot invade when unfavorable patches are large by moving slowly through them (fig. 1*D*), nor will an invasion slow down when movement in bad patches is fast (fig. 5; Shigesada et al. 1986). This difference arises since movement into and within patches was coupled in previous studies but not in ours. Persistence is ensured by entering bad patches at a low rate, not by moving slowly there. An invasion slows because of frequent movement into bad patches, not because of fast movement there.

Finally, when individuals move faster in less favorable habitat with $r > 0$, increasing the size of less favorable habitat may unexpectedly speed up an invasion (fig. 4). Hence, barrier zones (Sharov and Liebhold 1998) are effective to control invasions only if growth potential is sufficiently low there; otherwise, an invasion may move faster.

These results provide strong theoretical evidence for the importance of including detailed movement behavior at interfaces in population models. Empirical evidence comes

from fitting harvesting data for marine protected areas (Langebrake et al. 2012). Different ecological situations will require different conditions, and we hope that our results will spark empirical work to test different scenarios. For example, one could impose a particular step size by varying spacing between host plants (Turchin 1998, p. 79) while keeping the overall density constant. Alternatively, one could impose temporal movement restrictions to vary movement rates while keeping the spacing of host plants constant.

Effects of Patch Preference

Patch preference (α) introduces into reaction-diffusion models behavioral details that could not be included previously (but see Cantrell and Cosner 1999). Individuals preferentially choose patches for such reasons as higher resource quality or abundance (Brown 1988; Fryxell 2008) and lower predation risk (Brown 1988; Verdolin 2006). Qualitatively, patch preference affects persistence and spread in a relatively predictable way, but our model provides quantitative and sensitivity results. Minimal patch size decreases as preference for the patch increases, and sensitivity to changes in α is greatest when α is either 0 or 1 (fig. A2). In a patchy landscape, a population can tolerate large bad patches if individuals have a strong-enough preference for favorable patches (fig. 2). The rate of spread is maximized at intermediate values of patch preference (fig. 6).

Patch preference helps understand the less intuitive results about differential movement from the expressions for jump size k in conditions (6) and (7). Faster movement in bad patches (higher D) and higher preference for good patches (higher α) both increase k. Hence, faster movement in unfavorable patches has an effect similar to that of higher preference for favorable patches. This observation intuitively explains some results on differential movement, but we caution against scaling motility and preference into a single parameter, since motility also affects population flux at an interface, whereas preference, at least in our formulation, does not.

How General Are These Results?

Cantrell and Cosner (1999) modeled habitat preference via "skew Brownian motion" (Walsh 1978), where habitat preference appears in the flux conditions at an interface. They studied persistence conditions for a species living in a protected core area surrounded by a buffer zone and found that a suitable buffer zone can reduce the required size of the core habitat. We implemented the same scenario with our interface conditions (see app. B, sec. B1, for details). The persistence conditions for our model differ from the ones found by Cantrell and Cosner (1999) only by a factor of D or $D^{1/2}$, depending on k. Hence, the results with respect to α are robust across model implementations, and we conjecture that there is some deeper mathematical connection between the two approaches than first meets the eye. In particular, the derivation of skew Brownian motion might depend on using Fickian flux or biological diffusion in reaction-diffusion models (Turchin 1998; Garlick et al. 2011).

More previous works on dynamics in patchy landscapes should be reexamined in the light of our findings. Conditions for invasion and coexistence between two competing microbes as derived by Cruywagen et al. (1996) will change, as will the results on persistence and invasion in advective environments (Lutscher et al. 2006; Vergni et al. 2012).

Our model is limited to a single spatial dimension and to local movement without temporal variation. Ovaskainen and Cornell (2003) also derive interface conditions in higher dimensions. For long-distance dispersal, one needs to start from an individual-level implementation of the mechanism, just as we did here. In our model, patch preference acts locally only at the interface. Kawasaki et al. (2012) modeled patch preference as attraction from greater distances. Some of their results are similar to ours (e.g., the hump-shaped dependence of c on α), but their model did not include differential movement.

Extensions

Ecologists gather a wealth of small-scale data on movement near interfaces and struggle to explain observations of population densities across edges (Ehrlich 1997; Lidicker 1999). Ries et al. (2004) present a qualitative model for mechanisms leading to positive, neutral, or negative edge effects. We suggest a mechanistic model that incorporates essential information about interface behavior, which was previously impossible in reaction-diffusion equations. We provide a detailed analysis of linear, low-density aspects. The one-dimensional setup could also be applied to corridor design (Andreassen et al. 1996). In the future, we will study nonlinear aspects, such as steady state distributions, and their profile across habitat edges. Some of these questions were already addressed when studying clines in genetics, at least for the continuous case (Nagylaki 1976; Slatkin 1973). We can study the effect of patch preference or differential movement on marginal population dynamics, thereby extending the work of Antonovics et al. (2006), who did not include these factors. Similarly, we suggest reexamining, with appropriate interface conditions, the work of Fagan et al. (2009) on how an Allee effect, together with critical patch size and gap-crossing ability, generates geographic range limits. Finally, we speculate that for interacting species, habitat preference could depend on a competitor or a predator. It will be partic-

ularly interesting to see how the results of Strohm and Tyson (2009) on the existence of limit cycles between predator and prey in fragmented habitats depend on the implementation of interface conditions. Ultimately, a full mechanistic understanding of the wealth of edge effects classified by Ries et al. (2004) will require integration of information across spatial and temporal scales. We suggest that this work is one crucial piece in that great puzzle.

Acknowledgments

We are grateful for inspiring discussions with C. Cobbold, M. Lewis, J. Musgrave, and O. Ovaskainen. We thank B. Fagan and two anonymous reviewers for valuable feedback. G.A.M. was supported by a grant from Foreign Affairs and International Trade Canada under the Emerging Leaders of the Americas program. F.L. is supported by a Discovery Grant from the Natural Sciences and Engineering Research Council of Canada.

Literature Cited

Andow, D., P. Kareiva, S. Levin, and A. Okubo. 1990. Spread of invading organisms. Landscape Ecology 4:177–188.

Andreassen, H., R. Ims, and O. Steinset. 1996. Discontinuous habitat corridors: effects on male root vole movements. Journal of Applied Ecology 33:555–560.

Antonovics, J., A. J. McKane, and T. J. Newman. 2006. Spatiotemporal dynamics in marginal populations. American Naturalist 167:16–27.

Artiles, W., P. G. S. Carvalho, and R. A. Kraenkel. 2008. Patch-size and isolation effects in the Fisher-Kolmogorov equation. Journal of Mathematical Biology 57:521–535.

Beyer, H. L., D. Haydon, J. Morales, J. Frair, M. Hebblewhite, M. Mitchell, and J. Matthiopoulos. 2010. The interpretation of habitat preference metrics under use-availability designs. Philosophical Transactions of the Royal Society B: Biological Sciences 365:2245–2254.

Brown, J. 1988. Patch use as an indicator of habitat preference, predation risk, and competition. Behavioral Ecology and Sociobiology 22:37–47.

Cantrell, R., and C. Cosner. 1999. Diffusion models for population dynamics incorporating individual behavior at boundaries: applications to refuge design. Theoretical Population Biology 55:189–207.

———. 2003. Spatial ecology via reaction-diffusion equations. Wiley, Chichester.

Cantrell, R., C. Cosner, and W. Fagan. 2012. The implications of model formulation when transitioning from spatial to landscape ecology. Mathematical Biosciences and Engineering 9:27–60.

Chapman, D., C. Dytham, and G. Oxford. 2007. Landscape and fine-scale movements of a leaf beetle: the importance of boundary behaviour. Oecologia (Berlin) 154:55–64.

Creegan, H., and P. Osborne. 2005. Gap-crossing decisions of woodland songbirds in Scotland: an experimental approach. Journal of Applied Ecology 42:678–687.

Crone, E., and C. Schultz. 2008. Old models explain new observations of butterfly movement at patch edges. Ecology 89:2061–2067.

Cruywagen, G., P. Kareiva, M. Lewis, and J. Murray. 1996. Competition in a spatially heterogeneous environment: modelling the risk of spread of a genetically engineered population. Theoretical Population Biology 49:1–38.

Debinski, D., and R. Holt. 2000. A survey and overview of habitat fragmentation experiments. Conservation Biology 14:342–355.

Dewhirst, S., and F. Lutscher. 2009. Dispersal in heterogeneous habitats: thresholds, spatial scales and approximate rates of spread. Ecology 90:1338–1345.

Ehrlich, P. 1997. A world of wounds: ecologists and the human dilemma. Ecology Institute, Oldendorf, Germany.

Fagan, W. F., R. S. Cantrell, and C. Cosner. 1999. How habitat edges change species interactions. American Naturalist 153:165–182.

Fagan, W. F., R. S. Cantrell, C. Cosner, and S. Ramakrishnan. 2009. Interspecific variation in critical patch size and gap-crossing ability as determinants of geographic range size distributions. American Naturalist 173:363–375.

Fahrig, L. 2007. Non-optimal animal movement in human-altered landscapes. Functional Ecology 21:1003–1015.

Fisher, R. 1937. The advance of advantageous genes. Annals of Eugenics 7:355–369.

Fryxell, J. M. 2008. Predictive modeling of patch use by terrestrial herbivores. Pages 105–124 *in* H. Prins and F. van Langevelde, eds. Resource ecology: spatial and temporal dynamics of foraging. Springer, Dordrecht.

Garlick, M., J. Powell, M. Hooten, and L. McFarlane. 2011. Homogenization of large-scale movement models in ecology. Bulletin of Mathematical Biology 73:2088–2108.

Hastings, A., K. Cuddington, K. Davies, C. Dugaw, A. Elmendorf, A. Freestone, S. Harrison, et al. 2005. The spatial spread of invasions: new developments in theory and evidence. Ecology Letters 8:91–101.

Kawasaki, K., K. Asano, and N. Shigesada. 2012. Impact of directed movement on invasive spread in periodic patchy environments. Bulletin of Mathematical Biology 74:1448–1467.

Kierstead, H., and L. B. Slobodkin. 1953. The size of water masses containing plankton blooms. Journal of Marine Research 12:141–147.

Langebrake, J., L. Riotte-Lambert, C. Osenberg, and P. De Leenheer. 2012. Differential movement and movement bias models for marine protected areas. Journal of Mathematical Biology 64:667–696.

Lidicker, W. J. 1999. Responses of mammals to habitat edges: an overview. Landscape Ecology 14:333–343.

Ludwig, D., D. G. Aronson, and H. F. Weinberger. 1979. Spatial patterning of the spruce budworm. Journal of Mathematical Biology 8:217–258.

Lutscher, F., M. Lewis, and E. McCauley. 2006. The effects of heterogeneity on population persistence and invasion in rivers. Bulletin of Mathematical Biology 68:2129–2160.

McKenzie, H., E. Merrill, R. Spiteri, and M. Lewis. 2012. How linear features alter predator movement and the functional response. Interface Focus 2:205–216.

Nagylaki, T. 1976. Clines with variable migration. Genetics 83:867–886.

Okubo, A., and S. A. Levin. 2001. Diffusion and ecological problems: modern perspectives. Springer, New York.

Ovaskainen, O. 2008. Analytical and numerical tools for diffusion-based movement models. Theoretical Population Biology 73:198–211.

Ovaskainen, O., and S. J. Cornell. 2003. Biased movement at a bound-

ary and conditional occupancy times for diffusion processes. Journal of Applied Probability 40:557–580.
Reeve, J., and J. Cronin. 2010. Edge behaviour in a minute parasitic wasp. Journal of Animal Ecology 79:483–490.
Reeve, J., J. Cronin, and K. Haynes. 2008. Diffusion models for animals in complex landscapes: incorporating heterogeneity among substrates, individuals and edge behaviours. Journal of Animal Ecology 77:898–904.
Ries, L., and D. Debinski. 2001. Butterfly responses to habitat edges in the highly fragmented prairies of central Iowa. Journal of Animal Ecology 70:840–852.
Ries, L., R. Fletcher Jr., J. Battin, and T. Sisk. 2004. Ecological responses to habitat edges: mechanisms, models, and variability explained. Annual Review of Ecology, Evolution, and Systematics 35: 491–522.
Robertson, O., and J. Radford. 2009. Gap-crossing decisions of forest birds in a fragmented landscape. Austral Ecology 34:435–446.
Rosenzweig, M. 1981. A theory of habitat selection. Ecology 62:327–335.
Schtickzelle, N., and M. Baguette. 2003. Behavioural responses to habitat patch boundaries restrict dispersal and generate emigration–patch area relationships in fragmented landscapes. Journal of Animal Ecology 72:533–545.
Schultz, C., and E. Crone. 2001. Edge-mediated dispersal behavior in a prairie butterfly. Ecology 82:1879–1892.
Sharov, A., and A. Liebhold. 1998. Model of slowing the spread of gypsy moth (Lepidoptera: Lymantriidae) with a barrier zone. Ecological Applications 8:1170–1179.
Shigesada, N., K. Kawasaki, and E. Teramoto. 1986. Traveling periodic waves in heterogeneous environments. Theoretical Population Biology 30:143–160.
Skellam, J. G. 1951. Random dispersal in theoretical populations. Biometrika 38:196–218.
Slatkin, M. 1973. Gene flow and selection in a cline. Genetics 75: 733–756.
Strohm, S., and R. Tyson. 2009. The effect of habitat fragmentation in cyclic population dynamics: a numerical study. Bulletin of Mathematical Biology 71:1323–1348.
Turchin, P. 1998. Quantitative analysis of movement: measuring and modeling population redistribution in animals and plants. Sinauer, Sunderland, MA.
Van Houtan, K., S. Pimm, J. Halley, R. Bierregaard Jr., and T. Lovejoy. 2007. Dispersal of amazonian birds in continuous and fragmented forest. Ecology Letters 10:219–229.
Van Kirk, R. W., and M. A. Lewis. 1999. Edge permeability and population persistence in isolated habitat patches. Natural Resource Modeling 12:37–64.
Verdolin, J. 2006. Meta-analysis of foraging and predation risk tradeoffs in terrestrial systems. Behavioral Ecology and Sociobiology 60: 457–464.
Vergni, D., S. Iannaccone, S. Berti, and M. Cencini. 2012. Invasions in heterogeneous habitats in the presence of advection. Journal of Theoretical Biology 301:141–152.
Walsh, J. 1978. A diffusion with discontinuous local time. Astérisque 52–53:37–45.
Weinberger, H. F. 1982. Long-time behavior of a class of biological models. SIAM Journal on Mathematical Analysis 13:353–396.
———. 2002. On spreading speeds and traveling waves for growth and migration models in a periodic habitat. Journal of Mathematical Biology 45:511–548.
Whittington, J., C. St. Clair, and G. Mercer. 2005. Spatial responses of wolves to roads and trails in mountain valleys. Ecological Applications 15:543–553.
With, K. 2002. The landscape ecology of invasive spread. Conservation Biology 16:1192–1203.

Associate Editor: Sean H. Rice
Editor: Troy Day

"The Mule Deer ... was first mentioned by Lewis and Clark in the report of their journey up the Missouri River. They gave it the name of Mule Deer on account of the length of its ears; the length of the ear, however, varies with individuals. ... This deer is found from the north of New Mexico to the Saskatchewan, and from the Missouri to the Cascade Mountains." From "The Mule Deer" by W. J. Hays (*American Naturalist*, 1869, 3:180–181).

 DOI: 10.1086/670661

Appendix A from G. A. Maciel and F. Lutscher, "How Individual Movement Response to Habitat Edges Affects Population Persistence and Spatial Spread"

(Am. Nat., vol. 182, no. 1, p. 000)

Mathematical Derivation and Analysis

A1. Derivation of Interface Conditions

In this appendix, we show how to generalize the work of Ovaskainen and Cornell (2003) and derive interface conditions (4). The different values of k then result from different assumptions about the behavior and random walk characteristics.

We consider an individual moving along a straight line in discrete time steps. We take position $x = 0$ as the interface between two different habitat types, labeled 1 (for $x > 0$) and 2 (for $x < 0$). Inside habitat type i, individuals may jump distance Δx_i to the right or left with equal probability per time step. At the interface, individuals move to patch 1 with probability α_1 and to patch 2 with probability α_2. An individual will remain at the interface with probability $1 - \alpha_1 - \alpha_2$.

Given these assumptions, we have the following master equation for the probability density function $P(-\Delta x_2, t)$, $P(0, t)$, and $P(\Delta x_1, t)$, which represent the probability per unit length of finding an individual at positions $-\Delta x_2$, 0, and Δx_1, respectively:

$$\Delta x_2 P(-\Delta x_2, t + \Delta t) = \frac{p_2}{2}\Delta x_2 P(-2\Delta x_2, t) + (1 - p_2)\Delta x_2 P(-\Delta x_2, t) + \alpha_2 \Delta x_0 P(0, t), \tag{A1}$$

$$\Delta x_0 P(0, t + \Delta t) = \frac{p_2}{2}\Delta x_2 P(-\Delta x_2, t) + \frac{p_1}{2}\Delta x_1 P(\Delta x_1, t) + (1 - \alpha_1 - \alpha_2)\Delta x_0 P(0, t), \tag{A2}$$

$$\Delta x_1 P(\Delta x_1, t + \Delta t) = \frac{p_1}{2}\Delta x_1 P(2\Delta x_1, t) + (1 - p_1)\Delta x_1 P(\Delta x_1, t) + \alpha_1 \Delta x_0 P(0, t), \tag{A3}$$

where Δx_1 and Δx_2 are the step lengths in patch types 1 and 2 and p_1 and p_2 are the respective probabilities of moving in each step.

We expand the terms on the left-hand side in Taylor series of Δt and terms containing $2\Delta x_1$ and $2\Delta x_2$ in series of Δx_1 and Δx_2. We obtain the equations

$$\Delta x_2 P(-\Delta x_2, t) = \frac{p_2}{2}\Delta x_2 P(-\Delta x_2, t) + (1 - p_2)\Delta x_2 P(-\Delta x_2, t) + \alpha_2 \Delta x_0 P(0, t) + O((\Delta x_2)^2) + O(\Delta x_2 \Delta t) + \cdots, \tag{A4}$$

$$\Delta x_0 P(0, t) = \frac{p_2}{2}\Delta x_2 P(-\Delta x_2, t) + \frac{p_1}{2}\Delta x_1 P(\Delta x_1, t) + (1 - \alpha_1 - \alpha_2)\Delta x_0 P(0, t) + O(\Delta x_0 \Delta t) + \cdots, \tag{A5}$$

$$\Delta x_1 P(\Delta x_1, t) = \frac{p_1}{2}\Delta x_1 P(\Delta x_1, t) + (1 - p_1)\Delta x_1 P(\Delta x_1, t) + \alpha_1 \Delta x_0 P(0, t) + O(\Delta x_1 \Delta t) + O((\Delta x_1)^2) + \cdots. \tag{A6}$$

Now, multiplying equation (A4) by α_1 and equation (A6) by α_2 and then subtracting the resulting equations, after few algebraic manipulations we find the relation

$$\alpha_1 p_2 \Delta x_2 P(-\Delta x_2, t) = \alpha_2 p_1 \Delta x_1 P(\Delta x_1, t) + O((\Delta x_1)^2) + O((\Delta x_2)^2) + O(\Delta x_1 \Delta t) + O(\Delta x_2 \Delta t) + \cdots. \tag{A7}$$

Taking the parabolic limits as Δx_1, Δx_2, and Δt tend to 0, we find the interface condition

$$\alpha_1 p_2 \lim_{\Delta x_i \to 0} \left(\frac{\Delta x_2}{\Delta x_1}\right) P(0^-, t) = \alpha_2 p_1 P(0^+, t). \tag{A8}$$

Here, $0^{\pm}$ denotes the limit as x approaches 0 from above and below. Since individuals move independently, this relation is also valid for the population densities.

Continuous-interface conditions. If we assume that step sizes are the same in the two patch types ($\Delta x_1 = \Delta x_2$) and that individuals move into a patch with the same probability as left or right within a patch ($\alpha_i = p_i/2$), we get the continuity condition

$$P(0^-, t) = P(0^+, t). \tag{A9}$$

This case was already derived by Nagylaki (1976).

Discontinuous-interface conditions. We recall the definition of the diffusion coefficient in each patch as $D_i = \lim_{\Delta t, \Delta x_i \to 0} [p_i \Delta x_i^2/\Delta t]$. If we assume $\Delta x_1 = \Delta x_2$, we can simply multiply both sides of equation (A8) by $\Delta x_1^2/\Delta t$ and arrive at condition (7). If instead $p_1 = p_2$, we obtain an additional factor $\Delta x_1/\Delta x_2$, which can be expressed via diffusion coefficients as $(D_1/D_2)^{1/2}$, so that we arrive at condition (6).

A condition for the derivatives of the population density at the interface can be derived by writing the following relation between fluxes:

$$D_1 \frac{\partial u_1}{\partial x}(\Delta x_1, t) - D_2 \frac{\partial u_2}{\partial x}(-\Delta x_2, t) = D_1 \frac{u_1(2\Delta x_1, t) - u_1(\Delta x_1, t)}{\Delta x_1} + D_2 \frac{u_2(-2\Delta x_2, t) - u_1(-\Delta x_2, t)}{\Delta x_2}. \tag{A10}$$

From relations (A3) and (A1), after expanding and rearranging terms we have

$$u_1(2\Delta x_1, t) - u_1(\Delta x_1, t) = u_1(\Delta x_1, t) - \alpha_1 \frac{\Delta x_0}{\Delta x_1} \frac{2}{p_1} u_0(0, t), \tag{A11}$$

$$u_2(-2\Delta x_2, t) - u_2(-\Delta x_2, t) = u_2(-\Delta x_2, t) - \alpha_2 \frac{\Delta x_0}{\Delta x_2} \frac{2}{p_2} u_0(0, t). \tag{A12}$$

Substituting these relations in equation (A10), we have

$$D_1 \frac{\partial u_1}{\partial x}(\Delta x_1, t) - D_2 \frac{\partial u_2}{\partial x}(-\Delta x_2, t) = [\Delta x_1 p_1 u_1(\Delta x_1, t) + \Delta x_2 p_2 u_2(-\Delta x_2, t) - 2(\alpha_1 + \alpha_2)\Delta x_0 u_0(0, t)] \frac{1}{\Delta t}. \tag{A13}$$

Noting that the term between brackets is simply relation (A2), we find, after taking the limits of Δx_1 and Δx_2 tending to 0,

$$D_1 \frac{\partial u_1}{\partial x}(0^+, t) - D_2 \frac{\partial u_2}{\partial x}(0^-, t) = 0, \tag{A14}$$

which is the flux conservation in equation (7).

A2. Persistence Conditions for a Single Species in a Periodically Varying Environment

We present more detailed calculations that lead to the persistence conditions in an infinite, periodically alternating landscape, following Shigesada et al. (1986). The nonlinear, dimensional model is

$$\frac{\partial u_1}{\partial t} = D_1 \frac{\partial^2 u_1}{\partial x^2} + u_1(r_1 - \mu_1 u_1) \quad \text{(in favorable patches)}, \tag{A15}$$

$$\frac{\partial u_2}{\partial t} = D_2 \frac{\partial^2 u_2}{\partial x^2} + u_2(r_2 - \mu_2 u_2) \quad \text{(in unfavorable patches)}. \tag{A16}$$

After linearizing, the quadratic terms in u_i with factor μ_i disappear. We start by introducing the nondimensional variables,

$$T = r_1 t, \quad X = \sqrt{\frac{r_1}{D_1}} x, \quad D = \frac{D_2}{D_1}, \quad r = \frac{r_2}{r_1},$$

and write the linearized equations (for variables U_i) in nondimensional form,

$$\frac{\partial U_1}{\partial T} = \frac{\partial^2 U_1}{\partial X^2} + U_1 \quad \text{(in favorable patches)}, \tag{A17}$$

$$\frac{\partial U_2}{\partial T} = D \frac{\partial^2 U_2}{\partial X^2} + r U_2 \quad \text{(in unfavorable patches)}. \tag{A18}$$

Assuming exponential solutions $U_i(X,T) = e^{\lambda T}V_i(X)$ $(i = 1, 2)$, we get the equations

$$\frac{\partial^2 V_1}{\partial X^2} + (1-\lambda)V_1 = 0 \quad \text{(in favorable patches)}, \tag{A19}$$

$$\frac{\partial^2 V_2}{\partial X^2} - \frac{(-r+\lambda)}{D}V_2 = 0 \quad \text{(in unfavorable patches)}, \tag{A20}$$

which have solutions

$$V_1(X) = A\cos\left(\sqrt{1-\lambda}X\right) + B\sin\left(\sqrt{1-\lambda}X\right), \tag{A21}$$

$$V_2(X) = A'\cosh\left(\sqrt{\frac{-r+\lambda}{D}}X\right) + B'\sinh\left(\sqrt{\frac{-r+\lambda}{D}}X\right).$$

Since this problem is periodic in space, it reduces to one period only, and interface conditions (4) become

$$V_1(0^+) = kV_2(0^-), \quad \frac{\partial V_1}{\partial X}(0^+) = D\frac{\partial V_2}{\partial X}(0^-), \tag{A23}$$

$$V_1(S_1^-) = kV_2(-S_2^+), \quad \frac{\partial V_1}{\partial X}(S_1^-) = D\frac{\partial V_2}{\partial X}(-S_2^+), \tag{A24}$$

where $S_1 = (r_1/D_1)^{1/2}L_1$ and $S_2 = (r_1/D_1)^{1/2}L_2$ are the nondimensional patch sizes.

Alternatively, one can use periodicity and symmetry and write conditions (A24) equivalently as

$$\frac{\partial V_1}{\partial X}(S_1/2) = 0 = \frac{\partial V_2}{\partial X}(-S_2/2). \tag{A25}$$

From these interface conditions, we find a linear system of four equations for parameters A, A', B, and B'. A positive solution exists if the determinant of the system vanishes. This condition leads to the following equation for λ:

$$\sqrt{1-\lambda}\tan\left(\sqrt{1-\lambda}\frac{S_1}{2}\right) = \frac{\sqrt{(-r+\lambda)D}}{k}\tanh\left(\sqrt{\frac{-r+\lambda}{D}}\frac{S_2}{2}\right). \tag{A26}$$

The persistence boundary is given by setting $\lambda = 0$. We derived these conditions under the assumption that unfavorable patches are characterized by a negative growth rate, so that $r < 0$. When $0 < r_2 < r_1$, so that unfavorable patches still allow for population growth, the square roots on the right-hand side of equation (A26) become purely imaginary. The same trigonometric identities as in Shigesada et al. (1986) can be used to obtain a real-valued equation.

In the main text, we illustrate how the persistence boundary depends on growth rate and patch size for different values of D. As a function of the two patch sizes, the order of the persistence boundaries with respect to interface conditions with $D > 1$ (fig. 1*C*) is reversed when $D < 1$ (fig. A1). Figure A2 shows how the minimal size of an isolated patch decreases with patch preference.

A3. Minimal Speed of Traveling Waves

We follow the calculations in Shigesada et al. (1986) to find the minimal traveling wave speed. We seek traveling periodic waves of the linearized system of the form

$$U(X,T) = f(Z)g(X), \quad Z = X - CT \quad (C = S/T^*), \tag{A27}$$

where C is the velocity of the propagating wave front and S is the spatial period ($S = S_1 + S_2$). T^* is the time required for the front to travel one spatial period. We further require that $f(Z) \to 0$ as $Z \to \infty$ and that $g(X) = g(X + S)$. As above, we write $g = g_{1,2}$ on favorable and unfavorable patches, respectively. Inserting equation (A27) into equations (A17) and (A18), we find $f(Z) = Ae^{-sZ}$ and

$$g_1'' - 2sg_1' + (1 + s^2 - Cs)g_1 = 0, \tag{A28}$$

$$g_2'' - 2sg_2' + \frac{(r + Ds^2 - Cs)}{D}g_2 = 0, \tag{A29}$$

where s is a damping factor. Matching conditions at interface points X_n are

$$\lim_{X\to X_n} g_1(X) = \lim_{X\to X_n} kg_2(X), \tag{A30}$$

$$\lim_{X\to X_n} (g_1'(X) - sg_1(X)) = \lim_{X\to X_n} D(g_2'(X) - sg_2(X)). \tag{A31}$$

Solving the equations for $g_i(X)$ with these interface conditions, we find the dispersion relation

$$\cosh s(S_1 + S_2) = \cosh(q_1S_1)\cosh(q_2S_2) + \frac{(q_1^2k^2 + q_2^2D^2)}{2Dq_1q_2k}\sinh(q_1S_1)\sinh(q_2S_2), \tag{A32}$$

where $q_1 = (Cs - 1)^{1/2}$ and $q_2 = [(Cs - r)/D]^{1/2}$.

Thus, given a fixed set of parameters, C relates to s through this condition. We observe that C is a convex function of s, so that a minimum speed, $C_{\min}$, exists. We illustrate how this minimum speed depends on parameters. Below, we show that the minimum speed is the actual spreading speed for the nonlinear equation.

We illustrate the dependence of the spreading speed on parameters r (fig. 4) and D (fig. 5) for continuous ($k = 1$) and discontinuous 1 (k as in eq. [6]) interface conditions in the main text. Comparison with figure A3 shows that the results for discontinuous 1 and 2 interface conditions are qualitatively similar. Figure A4 shows the dependence on r in the reverse case $D < 1$ for all interface conditions. Figures A5 and A6 illustrate the dependence of c on the size of bad patches.

Minimal Speed of the Linear Model and Asymptotic Spreading Speed of the Nonlinear Model

The minimal speed of the linear model (eq. [A18]) is an upper bound of the asymptotic spreading speed of the nonlinear model (eq. [A16]) because the nonlinear functions $u_i(r_i - \mu_i u_i)$ are bounded by their linearization at 0, r_iu_i. To show that the linearization at low density indeed gives the correct spreading speed for the nonlinear equations, we employ the analysis of Weinberger (2002). The theory by Weinberger applies to periodically heterogeneous habitats where the density function u for the species is continuous. Because of the interface conditions, the density function u in our model is not continuous for $k \neq 1$. Therefore, we rescale the density in patch type 2 by $1/k$, that is, we set $w_1 = u_1$ and $w_2 = ku_2$. Then the resulting equations for w_i are continuous at the interfaces. Hence, the results by Weinberger (2002) guarantee that the asymptotic spreading speed coincides with the minimum speed of the linearized equations. In particular, the asymptotic spreading speed is independent of the carrying capacities of the species in the different patch types.

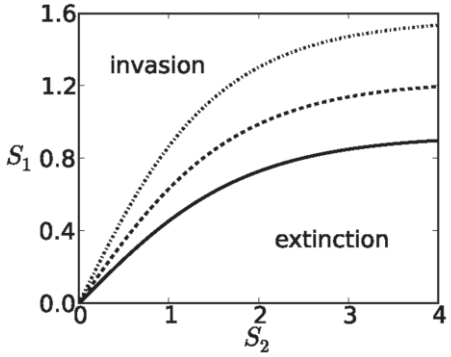

Figure A1: Persistence conditions (10) as a function of patch sizes S_1 and S_2. The three curves correspond to $k = 1$ (solid curve), k as in condition (6) (dashed curve), and k as in condition (7) (dash-dot curve). Fixed parameters are $D = 0.5$ and $r = -0.5$. We assume that individuals show no habitat preference, so that $\alpha = 0.5$.

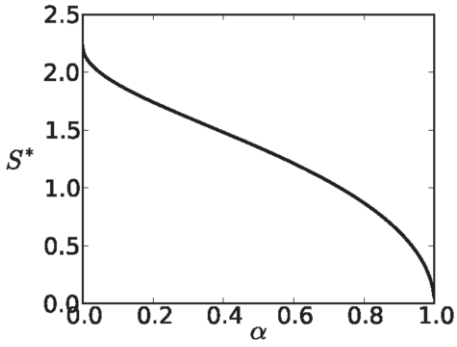

Figure A2: Minimal patch size as a function of probability α of moving to the focal patch. Choosing $D = 1$, the expressions for discontinuous 1 and discontinuous 2 are identical. Parameter values are $D = 1$ and $r = -2$.

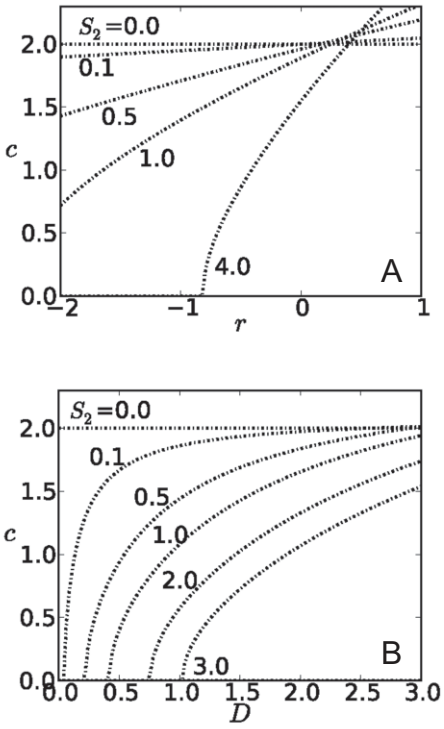

Figure A3: Spread rates as a function of intrinsic growth rate (*A*) or diffusivity (*B*) in unfavorable patches for interface condition (7). Parameters are $D = 2$, $S_1 = 1$, and $\alpha = 0.5$.

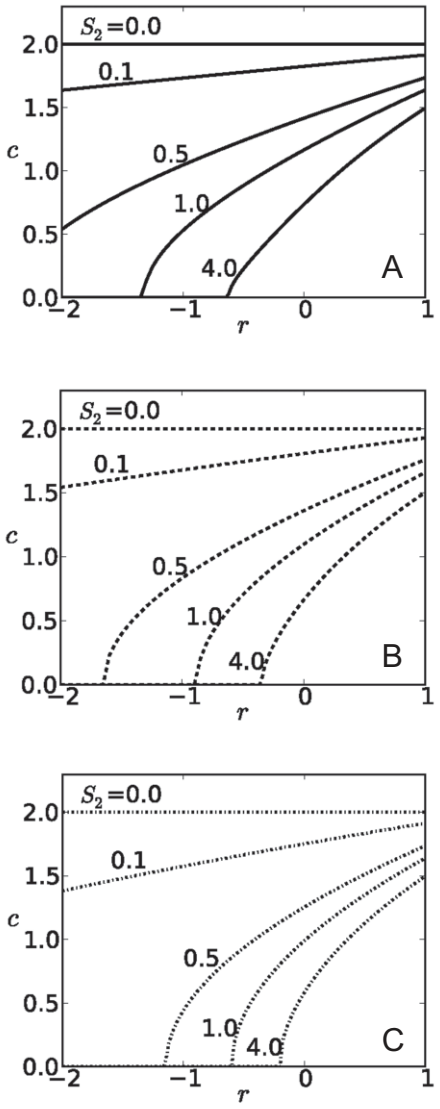

Figure A4: Spread rates as a function of intrinsic growth rate in the unfavorable patch. *A* corresponds to continuous density at interfaces ($k = 1$), *B* corresponds to discontinuous density as in condition (6), and *C* reflects condition (7). Parameters are $D = 0.5$, $S_1 = 1$, and $\alpha = 0.5$.

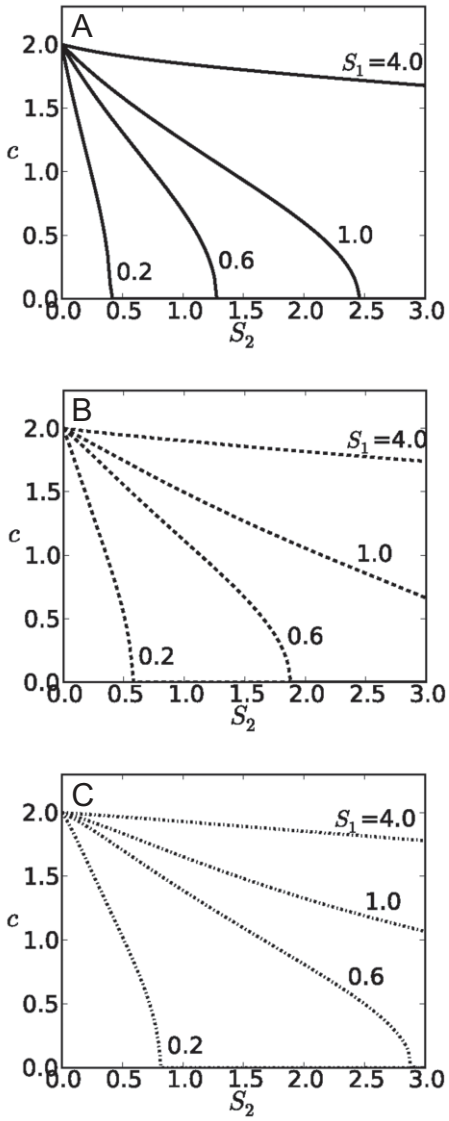

Figure A5: Spread rates as a function of size of unfavorable patches. *A* corresponds to continuous density at interfaces ($k = 1$), *B* corresponds to discontinuous density as in condition (6), and *C* reflects condition (7). Parameters are $D = 2$, $r = -0.5$, and $\alpha = 0.5$.

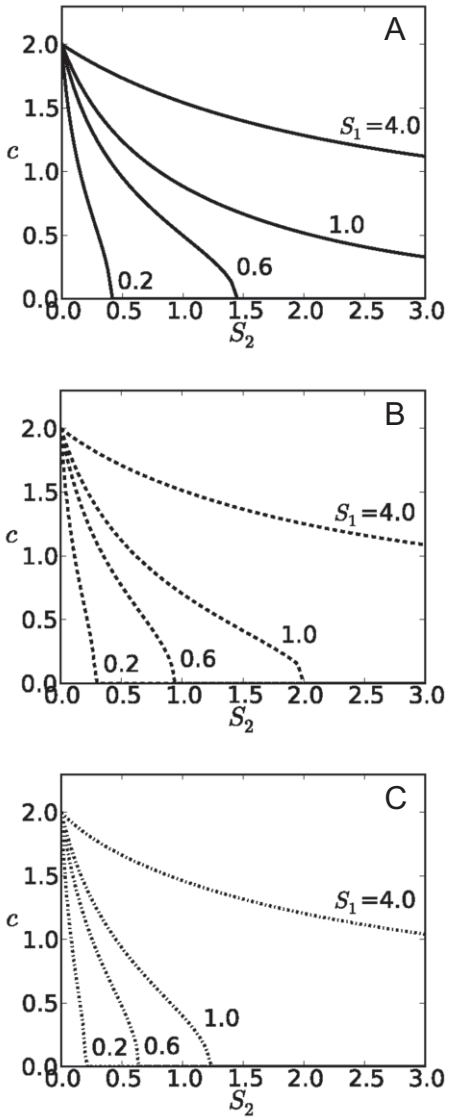

Figure A6: Same as figure A5, but with $D = 0.5$.

 DOI: 10.1086/670661

Appendix B from G. A. Maciel and F. Lutscher, "How Individual Movement Response to Habitat Edges Affects Population Persistence and Spatial Spread"

(Am. Nat., vol. 182, no. 1, p. 000)

Further Applications

B1. Applications to Refuge Design

Following Cantrell and Cosner (1999), we study a landscape that has a core habitat in which population growth is high, surrounded by a buffer zone where population growth is less than in the core. The buffer zone is, in turn, surrounded by hostile environment. In one spatial dimension, we represent this setup as a patch of size $2L_1$ of core habitat, with a patch of length L_2 attached at each end. To ease direct comparison with the work of Cantrell and Cosner (1999), we present the calculations in dimensional form here. Using the symmetry of the configuration, we need to consider only half the core habitat with one buffer attached. Hence, we have the model equation (Cantrell and Cosner 1999)

$$\begin{aligned}\frac{\partial u_1}{\partial t} &= D_1\frac{\partial^2 u_1}{\partial x^2} + r_1u_1(1-u_1), \quad 0<x<L_1\\ \frac{\partial u_2}{\partial t} &= D_2\frac{\partial^2 u_2}{\partial x^2} + r_2u_2(1-u_2), \quad -L_2<x<0.\end{aligned} \tag{B1}$$

At the boundary between the buffer and the hostile exterior, we have $u_2(-L_2, t) = 0$. At the center of the core habitat, symmetry requires the boundary condition $(\partial u_1/\partial x)(L_1,t) = 0$. At the interface between core and buffer, Cantrell and Cosner (1999) used the conditions

$$\begin{aligned}\left(D_2\frac{\partial^2 u_2}{\partial x^2} + r_2u_2\right)(0^-, t) &= \left(D_1\frac{\partial^2 u_1}{\partial x^2} + r_1u_1\right)(0^+, t),\\ (1-\alpha)D_2\frac{\partial u_2}{\partial x}(0^-, t) &= \alpha D_1\frac{\partial u_1}{\partial x}(0^+, t).\end{aligned} \tag{B2}$$

As in the main text, parameter α defines the preference of the core habitat.

We compare this approach with ours using interface conditions (4) as in the main text. To find persistence conditions, we linearize equations (B1) at low density and search for solutions of the form $u_i(x, t) = e^{\lambda t}f_i(x)$. On each of the two habitat parts, function f can be represented by a series of sine and cosine functions, that is, the eigenfunctions of the diffusion operator. The coefficients in the series expansion of f can be found by applying the interface conditions. After lengthy but standard calculations, we find that growth rate λ and model parameters are related by

$$\frac{(1-\alpha)}{\alpha}\frac{D_2}{D_1}\frac{\cot\left((r_1-\lambda/D_1)^{1/2}L_1\right)}{(r_1-\lambda/D_1)^{1/2}} = \frac{\tanh\left((\lambda-r_2/D_2)^{1/2}L_2\right)}{(\lambda-r_2/D_2)^{1/2}} \tag{B3}$$

in the model by Cantrell and Cosner (1999) and by

$$\frac{1}{k}\frac{D_2}{D_1}\frac{\cot\left((r_1-\lambda/D_1)^{1/2}L_1\right)}{(r_1-\lambda/D_1)^{1/2}} = \frac{\tanh\left((\lambda-r_2/D_2)^{1/2}L_2\right)}{(\lambda-r_2/D_2)^{1/2}} \tag{B4}$$

with our interface conditions. In particular, the persistence boundary is the curve obtained by setting $\lambda = 0$. (As for eq. [A26] before, we need to employ various trigonometric identities in case $r_2 > 0$.)

Recall that k contains the factor $\alpha/(1-\alpha)$. Therefore, somewhat surprisingly, even though habitat preference was implemented in very different ways, the two resulting implicit expressions for λ differ only by a factor of D_1/D_2 or $(D_1/D_2)^{1/2}$, depending on the choice of k.

Cantrell and Cosner (1999) showed graphically that increasing any of L_1, L_2, r_1, r_2, or α increases the growth rate (λ). These results still hold in the case of discontinuous interface conditions. The minimal size of the focal patch (L_1^*) as a function of diffusivities D_1 and D_2 is shown in figure B1. These results are similar to those from the section "Focal Patch

Surrounded by Matrix Habitat." In fact, as $L_2 \to \infty$, the two models are equivalent. When habitat preference α is a function of the difference in habitat quality ($r_1 - r_2$), Cantrell and Cosner (1999) found the somewhat counterintuitive result that increasing habitat quality in the buffer zone can decrease the population growth rate λ and thereby increase the minimal core length L_1^*. The same effect occurs with the interface conditions studied here.

B2. Applications to Reserve Networks

We consider the situation where a reserve consists of two favorable patches that are linked by a movement corridor. In one spatial dimension, we represent this setup as two patches of size L_1 with positive population growth rate ($r_1 > 0$), separated by a "corridor" patch of length L_2 with negative growth rate ($r_2 < 0$). We are interested in how the quality of the corridor affects persistence of the population.

We assume hostile boundary conditions at those ends of the favorable patches that do not border the corridor. At the interface between the favorable patches and the corridor, we impose interface conditions (4), as in the main text. This setup is similar to the one used by Cantrell et al. (2012) to study the effects of model formulation on persistence conditions.

Using the symmetry of the arrangement, we obtain the linearized equations

$$\begin{aligned} \frac{\partial u_1}{\partial t} &= D_1 \frac{\partial^2 u_1}{\partial x^2} + r_1 u_1, \quad 0 < x < L_1 \\ \frac{\partial u_2}{\partial t} &= D_2 \frac{\partial^2 u_2}{\partial x^2} + r_2 u_2, \quad -L_2/2 < x < 0. \end{aligned} \tag{B5}$$

The boundary conditions are $u_1(L_1, t) = 0$; symmetry leads to the condition $(\partial u_2/\partial x)(-L_2/2, t) = 0$, and interface conditions (4) are imposed at $x = 0$. Note that this system is very similar to the equations studied in the previous sections.

When $L_1 > \pi(D_1/r_1)^{1/2}$, each patch individually exceeds the critical patch size for hostile boundary conditions and the population will persist, independently of the presence of a corridor. When $2L_1 < \pi(D_1/r_1)^{1/2}$, then the combined size of the two favorable patches is below the critical patch size. Hence, even if the two patches are adjacent ($L_2 = 0$), the population will go extinct. Therefore, we choose $\pi(D_1/r_1)^{1/2}/2 < L_1 < \pi(D_1/r_1)^{1/2}$ and determine conditions on L_2, r_2, and movement parameters, under which the population can persist in the network of two patches and corridor.

When all other parameters are fixed, higher mortality in the corridor requires a shorter corridor for population persistence. However, if individuals increase their movement rate in the corridor as mortality increases, persistence requirements could become less severe. We explore this possibility by setting

$$D(|r_2|) = \frac{D_0(1 + \delta_1|r_2|)}{2D_0 + \delta_1|r_2|}, \tag{B6}$$

the same functional form as for patch preference α in the section "Patch Preference Depends on Patch Attributes." The results are illustrated in figure B2. With discontinuous interface conditions, the persistence region increases if individuals move faster due to higher mortality. However, with continuous interface conditions ($k = 1$), the persistence region decreases if individuals move faster because of higher mortality. Hence, again we find that the previously used interface conditions produce a counterintuitive result, since movement within and into the corridor are correlated.

Instead of increasing motility in the corridor, individuals could also respond to decreasing corridor quality by decreased use of the corridor, that is, increased preference for the good patches. We model this behavior by setting

$$\alpha(|r_2|) = \frac{\alpha_0(1 + \delta_2|r_2|)}{2\alpha_0 + \delta_2|r_2|}. \tag{B7}$$

This choice will increase persistence of the population somewhat if α_0 is below a certain threshold. Above that threshold, a population can persist for an arbitrarily large distance between the two good patches as long as the corridor quality is low enough (fig. B3). The explanation for this phenomenon is that high preference for a good patch will effectively create a no-flux boundary, and with no individuals lost through that part of the patch boundary, the population can persist.

The positive effects of increasing motility and patch preference as decreasing corridor quality give even more opportunity for population persistence (fig. B4).

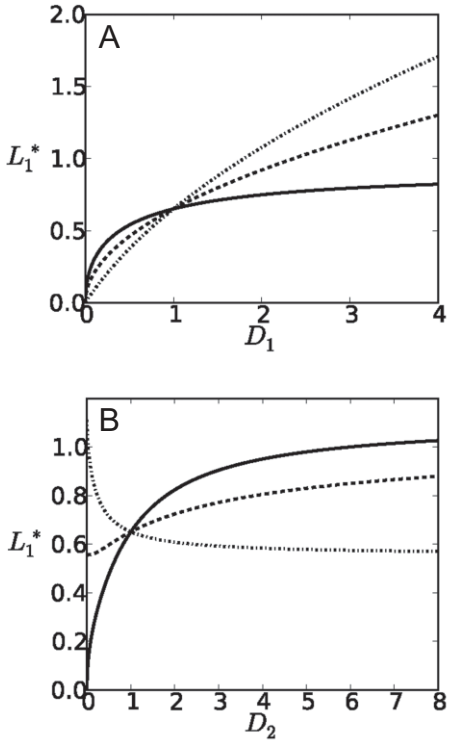

Figure B1: The critical length of the core habitat, surrounded by a buffer zone. The population persists for $L_1 > L_1^*$. The solid curve corresponds to $k = 1$, the dashed curve to k as in condition (6), and the dash-dot curve to k as in condition (7). The other parameters are $\alpha = 0.5$, $L_2 = 1$, $r_1 = 2$, and $r_2 = -1$. The plot in A has $D_2 = 1$, and the plot in B has $D_1 = 1$.

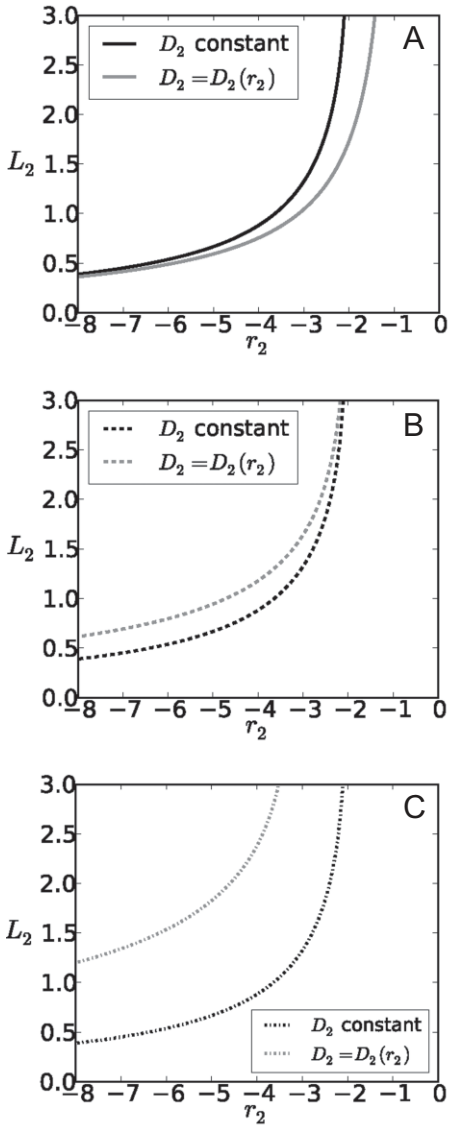

Figure B2: The critical length of the corridor between two favorable patches as a function of mortality in the corridor. The population persists for L_2 below the curve. The solid curves in *A* correspond to $k = 1$, the dashed curves in *B* correspond to k as in condition (6), and the dash-dot curves in *C* correspond to k as in condition (7). The black curves indicate constant $D_2 = 1$, whereas the gray curves represent D_2 varying with r_2. The other parameters are $\alpha = 0.5$, $r_1 = 2$, $D_1 = 1$, $D_0 = 5$, $\delta_1 = 1$, and $L_1 = 3\pi(D_1/r_1)^{1/2}/4$.

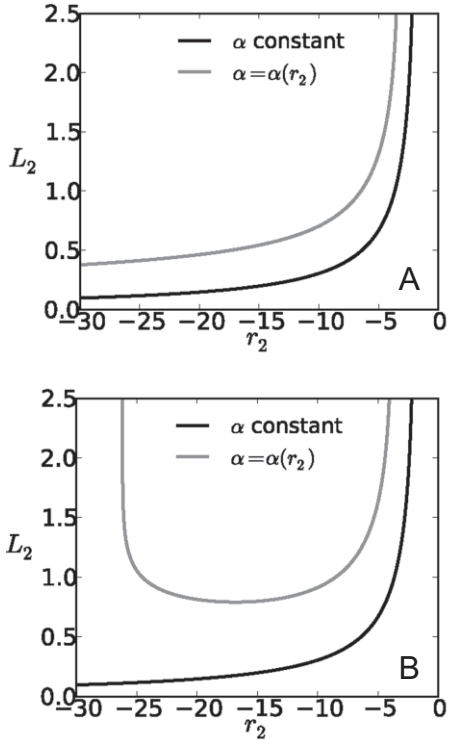

Figure B3: The critical length of the corridor between two favorable patches as a function of mortality in the corridor when patch preference depends on r_2. The population persists for L_2 below the curve. The black curves correspond to constant α, and the gray curves correspond to α as in equation (B7). The value $\alpha_0 = 0.9$ is below the threshold in *A*, and $\alpha_0 = 1$ is above it in *B*. Parameters are $\alpha = 0.5$ for black lines, $r_1 = 2$, $D_1 = D_2 = 1$, $\delta_2 = 0.1$, and $L_1 = 3\pi(D_1/r_1)^{1/2}/4$. Since $D_1 = D_2$, there is no difference between discontinuous 1 and 2 interface conditions.

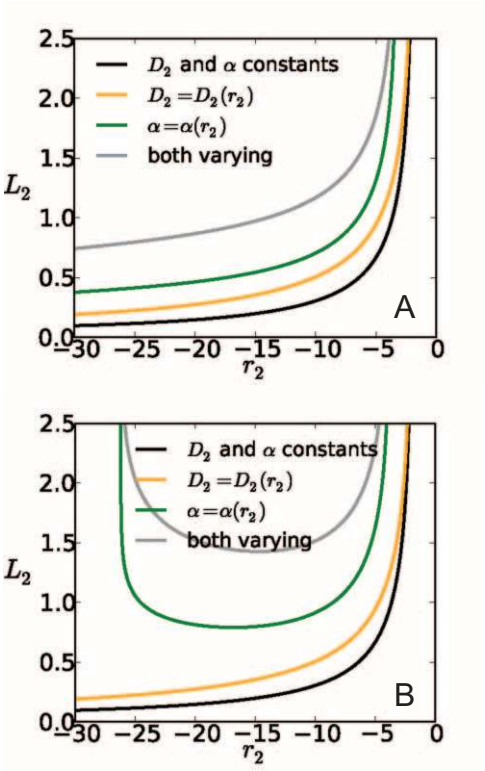

Figure B4: The critical length of the corridor between two favorable patches as a function of mortality in the corridor when patch preference and motility depend on r_2. The population persists for L_2 below the curve. The black curves correspond to constant α, and the yellow curves correspond to varying only D_2. The green curves arise when only α depends on r_2, and the gray curves arise when both parameters increase with $|r_2|$. The values are $\alpha_0 = 0.9$ in A and $\alpha_0 = 1$ in B. Other parameters are $D_0 = 5$, $r_1 = 2$, $D_1 = 1$, $\delta_1 = 1$, $\delta_2 = 0.1$, and $L_1 = 3\pi(D_1/r_1)^{1/2}/4$. The fixed parameters (where applicable) are $D_2 = 1$ and $\alpha = 0.5$. These plots are for the case of discontinuous 1 interface conditions.